A STUDY OF BOUNDARY LAYER FORMATION FROM A MOVING FLAT SURFACE USING LAGRANGIAN LARGE EDDY SIMULATION

Alex Mendonça Bimbato, alexbimbato@unifei.edu.br
Luiz Antonio Alcântara Pereira, luizantp@unifei.edu.br
Institute of Mechanical Engineering, Federal University of Itajuba, Av. BPS, 1303, CEP. 37500-903, Itajuba, MG, Brazil

Miguel Hiroo Hirata, hirata@fat.uerj.br
State University of Rio de Janeiro, FAT-UERJ, Resende, RJ, Brazil

Abstract. *The ground effect phenomenon has received a great deal of attention owing to its practical significance for the automotive industry. Results available in the literature has been shown that the mechanisms of ground effect are still far from being fully understood mainly due to the confusing influence of the boundary layer formed on the ground. Experimental results from Nishino (2007) reported that a ground running with the incoming flow velocity practically does not allow the development of boundary layer. Based on this experimental observation, a numerical implementation can be performed using a fixed ground, on which is necessary to impose only the impermeability condition on the ground surface. As consequence, a linear system of algebraic equations for the unknown vortex strengths is formed in order to ensure that the no-slip condition is satisfied and that circulation is conserved only on the body surface in the vicinity of a ground plane. In this paper are compared two versions of a Lagrangian vortex method implementation to simulate the two-dimensional, incompressible, unsteady flow around a circular cylinder in moving ground effect at a high Reynolds number: one based on the Nishino´s observation, and the other based on the model of a true moving ground. In the second case, the ground runs in a manner that one cycle of motion changes the co-ordinates of each panel that represents the ground surface, which travels at the same speed as the freestream. The true moving ground effect implementation imposes the impermeability and no-slip conditions on the body and ground plane surfaces. The method takes into account the sub-grid scale phenomena through a second-order velocity structure function adapted to the Lagrangian vortex method. Results are presented and calculations of the near wake show that the wake interference mechanism is present even for the true moving conditions of ground plane.*

Keywords. *Moving ground problem, Bluff body, Aerodynamic Forces, Vortex method, Sub-scale model.*

1. INTRODUCTION

Flows around bluff bodies include a variety of fluid dynamic phenomena, such as separation, vortex shedding and transition to turbulence, all of which stimulates scientific interest and has great impact in engineering applications. The problem of bluff body flows is applicable, for example, to the aerodynamic of road vehicle and the major interest came from motor racing companies. Cylinders having a two-dimensional structure permit that numerical and experimental investigations reveal the fundamental features of flows, where a moving ground situation is essential.

The characteristics of flow around a circular cylinder placed near and parallel to a plane boundary, or ground, are governed not only by the Reynolds number but also by gap ratio, i. e., the ratio of the gap between the cylinder and the ground, *h*, to the cylinder diameter *d*. However, the mechanisms of the ground effect are still far from being fully understood due to a variety of other influencing factors, in particular the confusing influence of the boundary layer formed on the ground.

One of the first investigations on the effects of the gap ratio *h/d* was carried out by Taneda (1965). He visualised the flow behind a circular cylinder toweed through stagnant water close to a stationary wall (i. e., the water and wall moving together relative to the cylinder and hence no boundary layer formed on the wall) at a very low Reynolds number of 170. His work showed that regular vortex shedding occurred at $h/d = 0.60$, whereas only a weak single row of vortices was generated at $h/d = 0.10$.

Roshko *et al*. (1975) measured the time-average drag and lift coefficients, C_D and C_L, for a circular cylinder placed near a fixed wall in a wind tunnel at $Re = 2.0\times10^4$, and showed that C_D rapidly decreased and C_L increased as the cylinder came close to the wall. Zdravkovich (2003) studied the drag behaviour for a circular cylinder placed near a moving ground running at the same speed as the freestream for a higher Reynolds number ($Re = 2.5\times10^5$), and verified that there was practically no boundary layer on the ground. The decrease in drag due to the decrease in *h/d* did not occur in his measurements. However, it was not clear whether this was attributed to the non-existence of the wall boundary layer or the higher Reynolds number, or any other influencing factors.

Nishino (2007) reproduced the same tests made by Zdravkovich (2003) for $Re = 4.0\times10^4$ and $Re = 1.0\times10^5$. The end conditions were taking into account by the use of end-plates in the cylinder extremities, in order to turn the flow approximately two-dimensional. When the end plates were not used (three-dimensional flow, essentially), the drag

coefficient increased as the gap ratio (*h/d*) decreased. Nishino (2007) attributes this behaviour to the non-formation of boundary layer on the ground.

Bimbato *et al*. (2009) used a Lagrangian vortex method to simulate numerically the particular situation studied experimentally by Nishino (2007) for the cylinder with end-plates at $Re = 1.0 \times 10^5$. Their numerical strategy fixed the ground and the vorticity generation was simulated only from the cylinder surface. As consequence, the moving ground effect was not taking into account effectively in their numerical simulations. Numerical results from Bimbato *et al.* (2009) included the time evolution of the lift and drag coefficients and the instantaneous pressure distributions for strategic chosen instants of the time evolution. This approach was very interesting and illustrated the near field wake which is important to understand the flow behaviour. However, the sub scale phenomena were not simulated.

Recently, Kamemoto (2009) presented an overview of development of vortex methods after 1960. He showed that the attractive features of Lagrangian vortex method are: (i) the discrete vortex method represents the vorticity by discrete vortices, whose transport at each time step is carried out in sequence to simulate convective and viscous diffusion process; (ii) grid-generation in a flow field is not necessary at all; (iii) use of RANS-type turbulence models is not necessary and (iv) moving or deforming boundary problems are easily dealt with.

More details of vortex methods are presented by Leonard (1980), Sarpkaya (1989), Lewis (1999), Kamemoto (2004), Stock (2007) and Hirata *et al*. (2008).

In the present paper a new numerical model of moving ground is presented and it is associated with a Lagrangian vortex method using Large Eddy Simulation (Alcântara Pereira *et al.*, 2002). The ground surface is represented by source flat panels (Katz and Plotkin, 1991) and with the dislocation of each flat panel; the ground is animate with a speed equal to the incident flow velocity. The code developed here, therefore, is an application to vortex flows of moving boundary problems. Numerical results from Bimbato *et al.* (2009) are reproduced here, using LES turbulence model, to be compared with true moving ground implementation.

Alcântara Pereira *et al.* (2004) observed that: "… the turbulence is essentially a 3-D phenomenon and yet one is modeling it using a 2-D approach; obviously it is then assumed 2-D turbulence. With this procedure one are still left with important turbulence aspects and the final results are also improved. The use of 2-D turbulence may explain some numerical results that depart from the experimental values".

2. GOVERNING EQUATIONS

Figure 1 presents schematically the two-dimensional unsteady and incompressible flow of a Newtonian fluid with constant properties which drain around a circular cylinder placed near a plane surface. The ground has the same speed as the oncoming flow. One can define: the incident flow (*U*); the semi-infinity fluid domain ($\Omega = S_1 \cup S_2 \cup S_3$), where S_1 is the body surface; S_2 is the plane surface and S_3 is the surface defined far from the body.

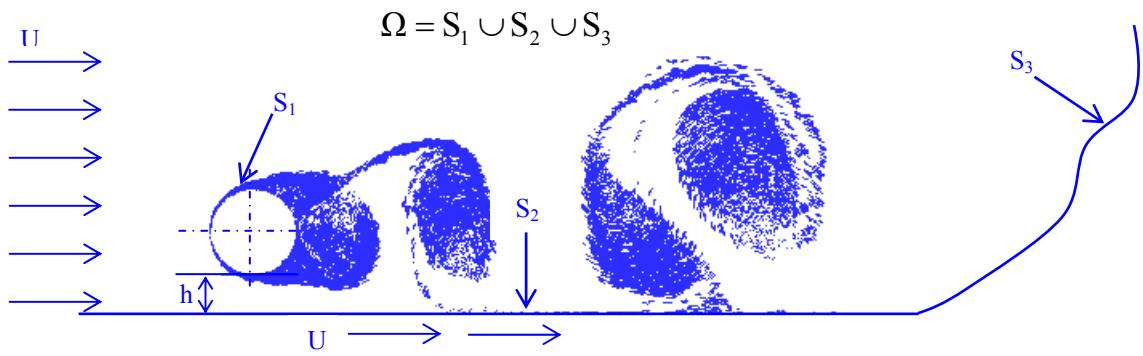

Figure 1. Definition of the fluid region

The problem is governed by equations (Alcântara Pereira *et al.*, 2002):

$$\frac{\partial \overline{u}_i}{\partial x_i} = 0\,, \tag{1}$$

where $\overline{u}$ is the velocity field filtered or the macro-scale field (Smagorinsky, 1963),

$$\frac{\partial \overline{u_i}}{\partial t} + \frac{\partial}{\partial x_j}\left(\overline{u_i}\,\overline{u_j}\right) = -\frac{1}{\rho}\frac{\partial \overline{p}}{\partial x_i} + 2\frac{\partial}{\partial x_j}\left[\left(\nu + \nu_t\right)\overline{S_{ij}}\right], \tag{2}$$

where $\overline{p}$ is the pressure field filtered, ρ is the density, ν is the molecular viscosity coefficient, ν_t is the eddy viscosity coefficient, and the deformation tensor of the filtered field is defined as:

$$\overline{S_{ij}} = \frac{1}{2}\left(\frac{\partial \overline{u_i}}{\partial x_j} + \frac{\partial \overline{u_j}}{\partial x_i}\right). \tag{3}$$

When using Lagrangian vortex method, the model proposed by Smagorinsky (1963) is inconvenient by the use of deformation rate (derivatives).

As an alternative, Métais and Lesieur (1992) considered that the small scales may not be too far from isotropic and proposed to use the local kinetic-energy spectrum $E_{(kc)}$ at the cut-off wave number (k_c) to define the eddy viscosity ν_t.

Using a relation given by Batchelor (1953), Lesieur and Métais (1996) proposed to calculate the local spectrum at k_c with a second-order velocity structure function $\overline{F_2}$ of the filtered field:

$$\overline{F_2}\left(\boldsymbol{x}, \Delta, t\right) = \left\| \overline{\boldsymbol{u}}\left(\boldsymbol{x}, t\right) - \overline{\boldsymbol{u}}\left(\boldsymbol{x} + \boldsymbol{r}, t\right) \right\|^2_{\|\boldsymbol{r}\| = \Delta}. \tag{4}$$

From the Kolmogorov spectrum the eddy viscosity can be written as a function of $\overline{F_2}$:

$$\nu_t\left(x, \Delta\right) = 0.105\, C_K^{-\frac{3}{2}}\, \Delta \sqrt{\overline{F_2}\left(\boldsymbol{x}, \Delta, t\right)}, \tag{5}$$

where $C_K = 1.4$ is the Kolmogorov constant.

In Eq. (4) is important to note that the "average operator" is applied in the velocities $\boldsymbol{u}\left(\boldsymbol{x} + \boldsymbol{r}, t\right)$ calculated under the surface of a sphere with center in $\boldsymbol{x}$ and radius $|\boldsymbol{r}|$.

The great advantage of the formulation presented above is the use of the concept of velocity fluctuation (differences) to be combined with Lagrangian vortex method.

Therefore, the strategy is to use the continuity equation, Eq. (1), and the Navier-Stokes equations, Eq. (2), to simulate the phenomena that occur in the macro-scales with the Lagrangian vortex method. The phenomena that occur in the micro-scales should be take into account through the eddy viscosity coefficient, Eq. (5); this coefficient (ν_t) is modeled with the second-order velocity structure function $\overline{F_2}$ of the filtered field, see Eq. (4).

It is necessary to impose the boundary conditions. The impenetrability condition demands that the normal velocity component of the fluid particle (u_n) should be equal to the normal velocities components of the surfaces S_1 and S_2 (v_n):

$$u_n - v_n = 0 \text{, on } S_1 \text{ and } S_2, \tag{6}$$

The no-slip condition demands that the tangential velocity component of the fluid particle (u_τ) should be equal to the tangential velocity component of the surface S_1 (v_τ), when there is no discrete vortex been generated under surface S_2 (Bimbato *et al.*, 2009):

$$u_\tau - v_\tau = 0 \text{, only on } S_1. \tag{7}$$

If the plane surface is animated with speed and discrete vortices are been generated under this surface, it must be written:

$$u_\tau - v_\tau = 0 \text{, on } S_1 \text{ and } S_2. \tag{8}$$

The last boundary condition to be imposed is that, far away, the perturbation caused by the solid boundaries fades as:

$$|\boldsymbol{u}| \to U \text{ , on } S_3 . \tag{9}$$

3. NUMERICAL SOLUTION: LAGRANGIAN VORTEX METHOD WITH LES SCHEME

The dynamics of the fluid motion is studied by taking the curl of the Eq. (2), obtaining the new 2-D vorticity equation (Alcântara Pereira *et al.*, 2002):

$$\frac{\partial \omega}{\partial t} + (\boldsymbol{u} \cdot \nabla)\omega = \frac{1}{Re_c} \nabla^2 \omega \text{ ,} \tag{10}$$

where the bars that identified the filtered field were omitted and the modified Reynolds number is defined in Eq. (14).

Chorin (1973) proposed the "Viscous Splitting Algorithm" to simplify the numerical implementation of the vortex method; with this algorithm, in the same time increment, the convective effects are solved independently of the viscous diffusion effects. In this way, the convective equation takes the well known Lagrangian form:

$$\frac{D\omega}{Dt} = 0 . \tag{11}$$

On the other hand, the diffusive equation is given by:

$$\frac{\partial \omega}{\partial t} = \frac{1}{Re_c} \nabla^2 \omega . \tag{12}$$

It is obvious from the equation above that the viscosity effects are taking into account in the diffusive process.

Alcântara Pereira *et al*. (2002) make two adaptations necessary to implement the second order structure function to the 2-D Lagrangian vortex method, see Eq. (4): (i) the points where the velocities must be calculated are placed inside a circular crown defined by $r_i = 0.1\sigma_0$ and $r_e = 2.0\sigma_0$, where r_i and r_e are the internal and external radius of the circular crown, respectively, and σ_0 is the Lamb vortex core of the vortex under analysis; (ii) to compute the second-order velocity structure function, the points where the velocities are calculated are the same as the positions of the vortices which are near the vortex under analysis and finally:

$$\overline{F_2} = \frac{1}{NV} \sum \left\| \boldsymbol{u}_t(\boldsymbol{x}) - \boldsymbol{u}_t(\boldsymbol{x} + \boldsymbol{r}_i) \right\|_i^2 \left(\frac{\sigma_0}{\boldsymbol{r}_i} \right)^{2/3} , \tag{13}$$

where $\boldsymbol{u}_t$ is the total velocity in the point, *NV* indicates the number of vortices inside the circular crown and r_i is the distance between the vortex under analysis and the vortices inside the circular crown.

In the sequence, the eddy viscosity coefficient is calculated making $\Delta = \sigma_0$ in Eq. (5). After this, the modified Reynolds number can be defined as:

$$Re_c = \frac{U\, d}{\nu + \nu_t} , \tag{14}$$

where *d* is the cylinder diameter and the dimensionless time is *d/U*. The Lamb vortex core is calculated as:

$$\sigma_{0_{\nu_t}} = 4.48364 \sqrt{\frac{\Delta t}{Re} \left(1 + \frac{\nu_t}{\nu} \right)} , \tag{15}$$

where Δt is the time increment of the numerical simulation.

To solve the convective problem, see Eq. (11), is necessary to determine the velocity field which is composed by three contributions: due to the incident flow $\boldsymbol{ui}(x,t)$, solid boundaries $\boldsymbol{ub}(\boldsymbol{x},t)$, and the vortex-vortex interaction $\boldsymbol{uv}(\boldsymbol{x},t)$. Thus:

$$\boldsymbol{u_i}(\boldsymbol{x},t) = \boldsymbol{ui}(\boldsymbol{x},t) + \boldsymbol{ub_i}(\boldsymbol{x},t) + \boldsymbol{uv_i}(\boldsymbol{x},t),\ i = 1,Z \tag{16}$$

where Z is the total number of Lamb discrete vortices in the wake.

The contribution of the incident flow is given by:

$$ui_1 = 1 \text{ and } ui_2 = 0\,. \tag{17}$$

The contribution of the solid boundaries is given by the source panel's method (Katz and Plotkin, 1991), so:

$$ub_i(x_j,t) = \sum_{k=1}^{NP} \sigma_k c_{jk}^i \left[x_j(t) - x_k\right],\ i = 1,2 \text{ and } j = 1,Z\,, \tag{18}$$

where NP is the number of flat panels that represents the solid boundaries, $\sigma_k = \text{const}$ is the density of sources per unit length and $c_{jk}^i\left(x_j(t) - x_k\right)$ is the i component of the velocity induced at discrete vortex j by k panel.

Finally, the contribution of the vortex cloud is given by:

$$uv_i(x_j,t) = \sum_{k=1}^{Z} \Gamma_k c_{jk}^i\left(x_j(t) - x_k(t)\right),\ i = 1,2 \text{ and } j = 1,Z\,, \tag{19}$$

where Γ_k is the intensity of the k vortex and $c_{jk}^i\left(x_j(t) - x_k\right)$ is the i component of the induced velocity in a discrete vortex j by a k discrete vortex.

With the velocity field, the convection is calculated by a first order Euler scheme:

$$\boldsymbol{x_i}(t + \Delta t) = \boldsymbol{x_i}(t) + \boldsymbol{u_i}\left(\boldsymbol{x_i}(t),t\right)\Delta t\,,\ i = 1,Z\,. \tag{20}$$

The diffusion equation, Eq. (12), is solved by the random walk scheme (Lewis, 1999), which consists in add a random displacement to Eq. (20):

$$\zeta_i(t) = \sqrt{\frac{4\,\Delta t}{Re_C} ln\left(\frac{1}{P}\right)}\left[cos2\,\pi\,Q + sen\,2\pi\,Q\right], \tag{21}$$

where P and Q are random numbers with $0 < P < 1$ and $0 < Q < 1$.

Once, with the vorticity field the pressure calculation starts with the Bernoulli function, defined by Uhlman (1992) as:

$$\overline{Y} = p + \frac{u^2}{2},\ u = |\boldsymbol{u}|\,. \tag{22}$$

Kamemoto (1993) used the same function and starting from the Navier-Stokes equations was able to write a Poisson equation for the pressure. This equation was solved using a finite difference scheme. Here the same Poisson equation was derived and its solution was obtained through the following integral formulation (Shintani and Akamatsu, 1994):

$$H\overline{Y_i} - \int_S \overline{Y}\nabla\Xi_i \cdot \boldsymbol{e_n}\,dS = \iint_\Omega \nabla\Xi_i \cdot (\boldsymbol{u}\times\boldsymbol{\omega})\,d\Omega - \frac{1}{Re}\int_S (\nabla\Xi_i \times \boldsymbol{\omega})\cdot \boldsymbol{e_n}\,dS\,, \tag{23}$$

where $H = 1$ in the fluid domain, $H = 0.5$ on the boundaries, Ξ is a fundamental solution of the Laplace equation and $\boldsymbol{e_n}$ is the unit vector normal to the solid surfaces.

The drag and lift coefficients are expressed by (see Bimbato, 2008):

$$C_D = -\sum_{k=1}^{NP} 2(p_k - p_\infty)\Delta S_k sen\beta_k = -\sum_{k=1}^{NP} C_p \Delta S_k sen\beta_k \ , \tag{24}$$

$$C_L = -\sum_{k=1}^{NP} 2(p_k - p_\infty)\Delta S_k cos\beta_k = -\sum_{k=1}^{NP} C_p \Delta S_k cos\beta_k \ , \tag{25}$$

where ΔS_k is the length and β_k is the angle and both of the k panel.

4. RESULTS AND DISCUSSION

4.1. Flow around an isolated circular cylinder

The flow past an isolated circular cylinder has been the object of considerable attention in preliminary numerical experiments to choose suitable values for: number of flat panels used to represent the circular cylinder ($NP = 300$), time increment ($\Delta t = 0.05$), core of a Lamb vortex ($\sigma_0 = 0.0010$). The distance ε off the panel where the new vortices are generated per time step is set equal to σ_0 for all the cases studied. More details are discussed in Bimbato (2008).

The time history of the aerodynamic forces, calculated from Eq. (24) and Eq. (25), is presented in Figure 2. The vortex shedding period can be seen in oscillations of the lift and drag coefficients. As soon as the numerical transient is over and the periodic steady state regime is reached (about 15 units of non-dimensional time) the drag coefficient oscillates two times more than the lift coefficient, which is a characteristic of an isolated circular cylinder. This means that for each vortex structure detachment, the lift coefficient completes a period, while the drag coefficient completes two periods.

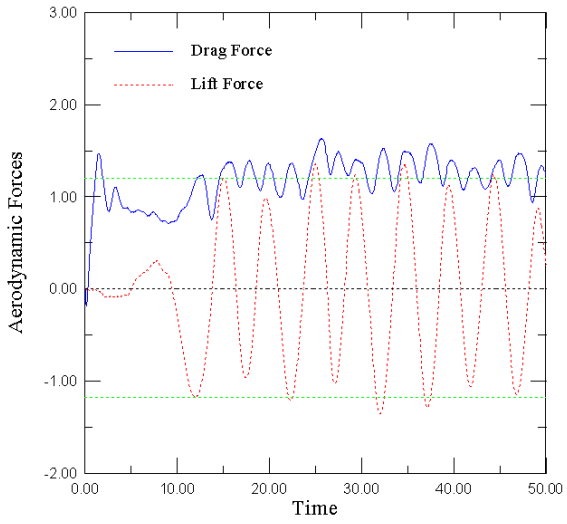

Figure 2. Time evolution of the aerodynamic forces for the isolated circular cylinder ($Re = 1.0 \times 10^5$)

The frequency of this detachment of vortices is measured by the Strouhal number, defined as:

$$St = \frac{f\,d}{U} \ , \tag{26}$$

where f is the detachment frequency of vortices.

Table 1 shows the comparison between the numerical results obtained by the Lagrangian vortex method with the experimental ones obtained by Blevins (1984), with $\pm 10\%$ of uncertainties. The numerical force coefficients are computed between $t_i = 25.40$ and $t_f = 49.30$ from Figure 2.

It can be observed that the drag coefficient is greater than the experimental value, which is a characteristic of two-dimensional simulations. The mean value of lift coefficient is not zero due to numerical errors.

Table 1. Isolated Circular Cylinder: Mean values of drag and lift coefficients and Strouhal number using LES model.

$Re = 1.0 \times 10^5$	$\overline{C_D}$	$\overline{C_L}$	$\overline{St}$
Blevins (1984)	1.20	-	0.19
Present Simulation	1.30	0.02	0.21

Figure 3 shows the position of the wake vortices for isolated circular cylinder at the last step of the computation ($t_f = 50.00$); the formation and shedding of large eddies in the wake is presented in accordance to the physics involved in the viscous flow. The present numerical simulation runs ended with 300,000 discrete vortices. The final CPU time was about 216h when using a Intel(R) Core(TM)2 Quad CPU, without parallel computation.

Figure 3. Position of the discrete vortices in the wake at $t_f = 50.00$ for an isolated circular cylinder ($Re = 1.0 \times 10^5$).

4.2. Flow around a circular cylinder in moving ground effect

The flow around a circular cylinder in ground effect presents several interesting characteristics, which can be described starting with the occurrence of the separation phenomenon.

Bimbato *et al*. (2009) analyzed the aerodynamic loads behaviour of a circular cylinder for $Re = 1.0 \times 10^5$ placed near a ground running at the same speed as the incident flow. As explained before, the ground surface was fixed and its motion was simulated by the suppression of the vorticity generation on it, since there is no velocity gradient between the ground and the freestream. It is important to emphasize that the vorticity generation on the cylinder surface was not suppressed, since there is a velocity gradient between the body and the freestream; so, the no-slip condition was verified just on the cylinder surface, see Eq. (7).

The numerical study reported in this paper is done to compare two distinct situations, defined as:

<u>*Situation 1*</u>: The numerical implementation made by Bimbato *et al*. (2009) adding here LES model (referred as *Case I* on Table 2).

<u>*Situation 2*</u>: A new Lagrangian vortex method implementation with LES model deal with moving boundary problem (referred as *Case II* on Table 2).

In the second situation above, the ground is running at the same speed as the freestream in a manner that its position is recalculated every time step. In this situation, the ground travels at the same speed as the incident flow and the impermeability and the no-slip boundary conditions on the ground surface are imposed. A numerical model of a moving ground plane is represented by a source distribution on the 200 panels, each of it with constant strength per unit panel length. For the moving conditions are computed the new-coordinates of each panel and instantaneous distance ε off the ground surface where the new vortices are generated in each time step.

Both situations are analyzed to conclude if the boundary layer developed on the ground is really negligible on this kind of ground effect problem, like Nishino (2007) says.

In all numerical results presented in Tab. 2, the gap-ratio is fixed in $h/d = 0.45$; see Fig. 1. This gap ratio is chosen to allow the comparison between the present numerical results with that ones approximately two-dimensional obtained by Nishino (2007); see details about the choice of this gap ratio ($h/d = 0.45$) in Bimbato (2008).

The results obtained for the drag coefficient show an acceptable discrepancy compared with the experimental value, referred as Nishino (2007); in both numerical situations, the lift coefficient is positive, but show great discrepancy compared with the experimental value. Additional investigations are necessary and will be presented elsewhere.

Table 2. Mean values of drag and lift coefficients and Strouhal number of a circular cylinder in ground effect for $h/d = 0.45$ at $Re = 1.0\times10^5$.

Authors	$\overline{C_D}$	$\overline{C_L}$	$\overline{St}$
Nishino (2007) with *end-plates*	1.311	0.102	-
Present result (*Case I*)	1.389	0.032	0.21
Present result (*Case II*)	1.418	0.287	0.20

Figure 4 shows the aerodynamic forces for both situations of $h/d = 0.45$; the force coefficients was averaged between $t_i = 27.45$ and $t_f = 47.50$, after the numerical transient reached.

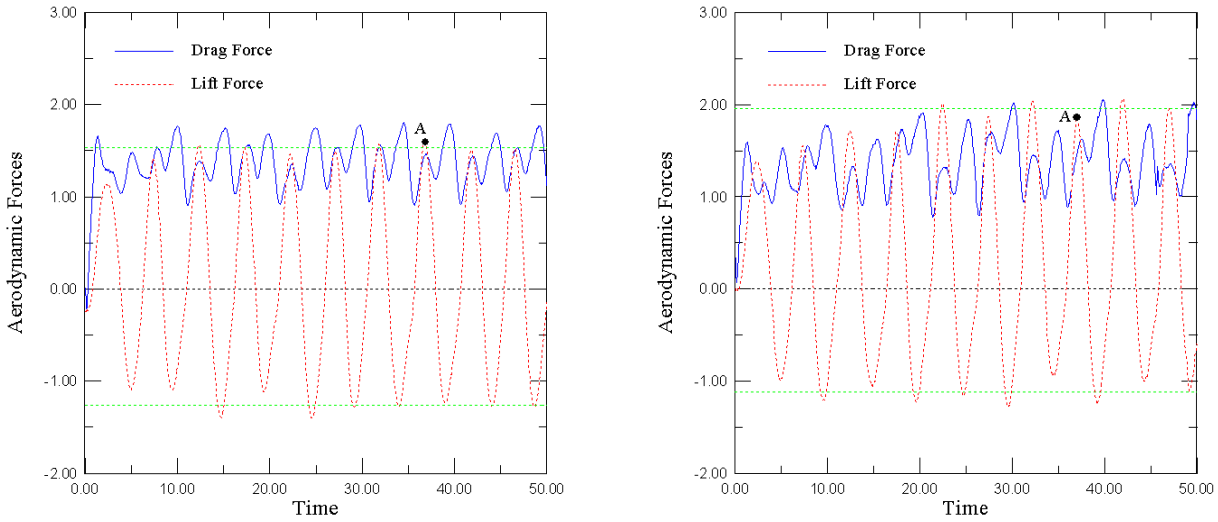

(a) *Case I* (b) *Case II*

Figure 4. Time evolution of the aerodynamic forces for a circular cylinder in ground effect ($h/d = 0.45$; $Re = 1.0\times10^5$)

Besides that the drag coefficient for the *Case I* is closer to the experimental value, one believes that the results referred in Tab. 2 as *Case II* is much more realistic. In fact, the analysis of the velocity field at an instant represented by point A (Fig. 5) shows that there is a boundary layer developed from the ground surface, when the ground effectively travels and vorticity is generated from the ground; see Fig. 5b.

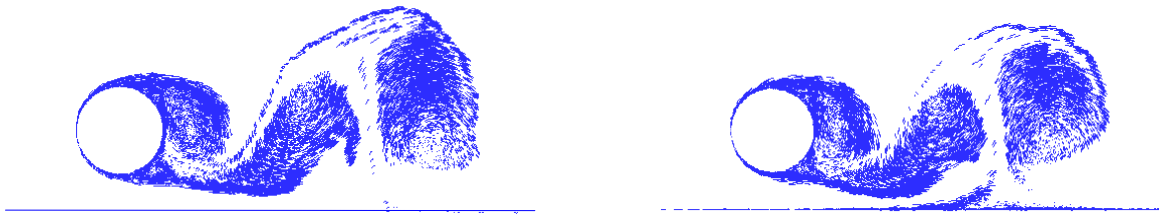

(a) *Case I* (b) *Case II*

Figure 5. Near field velocity distribution at an instant represented by point A ($h/d = 0.45$; $Re = 1.0\times10^5$).

In the Fig. 5b is clearly shown that the occurrence of separation on the cylinder surface contributes for the development of a boundary layer on the moving ground. However, the gap ratio adopted ($h/d = 0.45$) is not too small which causes a boundary layer not so thick; this fact turns the observations made by Nishino (2007) acceptable and, consequently, the results obtained by Bimbato (2008) and Bimbato *et al.* (2009) trusty. This is confirmed by the numerical values for both drag coefficients in Tab. 2: they are different in approximately 2%.

In order to understand what happens in this more realistic situation, consider Fig. 4b. It can be noted that, differently from the isolated circular cylinder case, when the bluff body is placed near a moving ground the drag coefficient did not has a mean amplitude defined; see in Fig. 2. On the contrary, it can be seen alternate amplitudes, sometimes higher,

sometimes lower. The explanation for this fact is given by the first mechanism that governs the ground effect phenomenon: the blockage effect due to the ground plane (see Fig. 6).

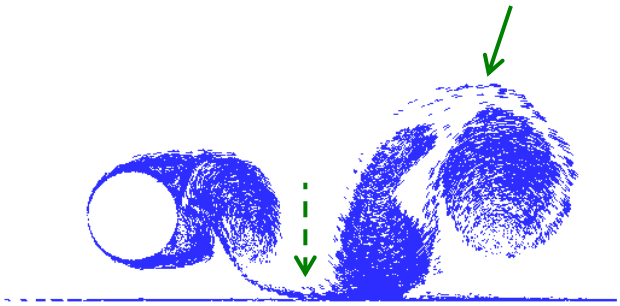

Figure 6. Near field velocity distribution (*Case II*; $h/d = 0.45$; $Re = 1.0 \times 10^5$)

The vortex structure pointed with continuous line has freedom to grow up, which contributes for the greater amplitudes of the drag coefficient in Fig. 4b. On the other hand, the vortex structure pointed with trace line has its development limited by the presence of the ground plane, which does not permit that the drag coefficient reaches bigger values, like occurs with the vortex structure pointed with continuous line. Due to the events above described the drag coefficient fit in greater and smaller amplitudes (see again Fig. 4b).

Finally, as one may observe in Fig. 7 the moving ground effect interferes effectively on the Von Kármán street formation. The present numerical simulation runs ended with 500,000 discrete vortices. The final CPU time was 628h 17min when using a Intel(R) Core(TM)2 Quad CPU, without parallel computation.

Figure 7. Position of the vortices in the wake at $t_f = 50.00$ for a circular cylinder in moving ground (*Case II*; $h/d = 0.45$; $Re = 1.0 \times 10^5$).

Comparing Fig. 3 with Fig. 7 it is easy to see the change on the wake structure. In Fig. 3 the wake seems to be formed by a series of "mushroom" type of vortex structure; analyzing Fig. 7 it can be seen that the vortex sheet that connects two larger vortex structures turns so smaller than that one that connects the bigger structures in the isolated circular cylinder. This characteristic will be more intense as the body come close to the ground.

5. CONCLUSIONS

A comparative numerical study of vortex shedding from a circular cylinder near a ground plane is performed to evaluate two versions of moving ground implementation using Lagrangian vortex method with LES turbulence model: one that uses a fixed ground and generates vorticity only from the circular cylinder surface (named as *Case I*) and another that uses a ground running at the same speed as the incident flow; as consequence, vorticity generation is necessary from the cylinder and moving ground surfaces (named as *Case II*). Our main conclusion is that the boundary layer developed on a moving belt of a wind tunnel can not be neglected even if the moving belt has the same speed as the oncoming flow. Additional investigations are necessary to elucidate the boundary layer effect formed on the ground for smaller gap ratios (h/d). However, small-gap regimes (h/d <0.35) are very difficult to investigate in a wind tunnel. The value for the drag coefficient predicted by the simulation using true moving ground effect (*Case II*) was, however, higher than numerical simulation using a fixed ground (*Case I*), and it needs further investigations.

Our Lagrangian vortex method developed here will be improved including parallel computation and furthermore the three dimensional effects present in the experiments, which are very important for the Reynolds number used in the simulations.

"Nowadays, applicability of the vortex element methods has been developed and improved dramatically, and it has become encouragingly clear that the vortex methods have so much interesting features that they provide researches and engineers with easy-to-handle and completely grid-free Lagrangian calculation of the unsteady and vortical flows without use of any RANS type turbulence models" (Kamemoto, 2009).

Finally, due to its various particularities and countless applications it is necessary many studies about the ground effect phenomenon in order to understand it better, especially the influence of other gap ratios and the roughness effect, which may be an important practical parameter that must be take into account on automobile competitions.

6. ACKNOWLEDGEMENTS

This research was supported by the CNPq (Brazilian Research Agency) Proc. 470420/2008-1, FAPEMIG (Research Foundation of the State of Minas Gerais) Proc. TEC APQ-01074-08 and FAPERJ (Research Foundation of State of Rio de Janeiro) Proc. E-26/112/013/08.

7. REFERENCES

Alcântara Pereira, L. A., Hirata, M. H., Manzanares Filho, N., 2004, "Wake and Aerodynamics Loads in Multiple Bodies – Application to Turbomachinery Blade Rows", J. Wind Eng. Ind. Aerodyn., 92, pp. 477-491.

Alcântara Pereira, L. A., Ricci, J. E. R., Hirata, M. H., Silveira Neto, A., 2002, "Simulation of the Vortex-Shedding Flow about a Circular Cylinder with Turbulence Modeling", CFD Journal, Vol. 11, No. 3, october, pp. 315-322.

Batchelor, G. K., 1953, "The Theory of Homogeneous Turbulence", Cambridge University Press.

Bimbato, A. M., Alcântara Pereira, L. A., Hirata, M. H., 2009, "Simulation of Viscous Flow around a Circular Cylinder near a Moving Ground", J. of the Braz. Soc. of Mech. Sci. & Eng., Vol. XXXI, No. 3, pp. 243-252.

Bimbato, A. M., 2008, Analysis of Moving Ground Effects on the Aerodynamic Loads of a Body, M.Sc. Dissertation, IEM/UNIFEI (in Portuguese).

Blevins, R. D., 1984, Applied Fluid Dynamics Handbook, Van Nostrand Reinhold, Co.

Chorin, A. J., 1973, "Numerical Study of Slightly Viscous Flow", Journal of Fluid Mechanics, Vol. 57, pp. 785-796.

Hirata, M. H., Alcântara Pereira, L. A., Recicar, J. N., Moura, W. H., 2008, "High Reynolds Number Oscillations of a Circular Cylinder", J. of the Braz. Soc. of Mech. Sci. & Eng., Vol. XXX, No. 4, pp. 300-308.

Kamemoto, K., 2009, "Perspective Characteristics of a Lagrangian Vortex Method in Application into Vortex Flows of Moving Boundary Problems", Workshop – From fast cars to slow flows over bluff bodies, 20-30 June, Imperial College, London, UK.

Kamemoto, K., 2004, "On Contribution of Advanced Vortex Element Methods Toward Virtual Reality of Unsteady Vortical Flows in the New Generation of CFD", Proceedings of the 10th Brazilian Congress of Thermal Sciences and Engineering-ENCIT 2004, Rio de Janeiro, Brazil, Nov. 29 - Dec. 03, Invited Lecture-CIT04-IL04.

Kamemoto, K., 1993, "Procedure to Estimate Unstead Pressure Distribution for Vortex Method" (In Japanese), Trans. Jpn. Soc. Mech. Eng., Vol. 59, No. 568 B, pp. 3708-3713.

Katz, J. and Plotkin, A., 1991, "Low Speed Aerodynamics: From Wing Theory to Panel Methods", McGraw Hill, Inc.

Leonard, A., 1980, "Vortex Methods for Flow Simulation", J. Comput. Phys., Vol. 37, pp. 289-335.

Lesieur, M. and Métais, O., 1996, "New trends in large-eddy simulation of turbulence". A Review in Fluid Mechanics, Vol. 28, pp. 45-82.

Lewis, R. I., 1999, "Vortex Element Methods, the Most Natural Approach to Flow Simulation - A Review of Methodology with Applications", Proceedings of 1st Int. Conference on Vortex Methods, Kobe, Nov. 4-5, pp. 1-15.

Métais, O. and Lesieur, M., 1992, "Spectral Large-Eddy Simulations of Isotropic and Stably-Statified Turbulence", J. Fluid Mech., 239, pp. 157-194.

Nishino, T., 2007, Dynamics and Stability of Flow Past a Circular Cylinder in Ground Effect, Ph.D. Thesis, Faculty of Engineering, Science and Mathematics, University of Southampton, 145p.

Roshko, A., Steinolfson, A. and Chattoorgoon, V., 1975, "Flow Forces on a Cylinder near a Wall or near another Cylinder", Proceedings of the 2nd U.S. National Conference on Wind Engineering Research, Fort Collins, Paper IV-15.

Sarpkaya, T., 1989, "Computational Methods with Vortices - The 1988 Freeman Scholar Lecture", Journal of Fluids Engineering, Vol. 111, pp. 5-52.

Shintani, M. and Akamatsu, T., 1994, "Investigation of Two Dimensional Discrete Vortex Method with Viscous Diffusion Model", Computational Fluid Dynamics Journal, Vol. 3, No. 2, pp. 237-254.

Smagorinsky, J., 1963, "General circulation experiments with the primitive equations", Mon. Weather Rev. 91,3,0099-164.

Stock, M. J., 2007, "Summary of Vortex Methods Literature (A lifting document rife with opinion)", April, 18: © 2002-2007 Mark J. Stock.

Taneda, S. (1965), "Experimental Investigation of Vortex Streets", Journal of the Physical Society of Japan, Vol. 20, pp. 1714-1721.

Uhlman, J. S., 1992, "An Integral Equation Formulation of the Equation of an Incompressible Fluid", Naval Undersea Warfare Center, T.R. 10-086.

Zdravkovich, M. M., 2003, Flow around Circular Cylinders: Vol. 2: Applications, Oxford University Press, Oxford, UK.

8. RESPONSIBILITY NOTICE

The authors are the only responsible for the printed material included in this paper.